

## Supplemental material

Di Biase et al., <https://doi.org/10.1084/jem.20182044>

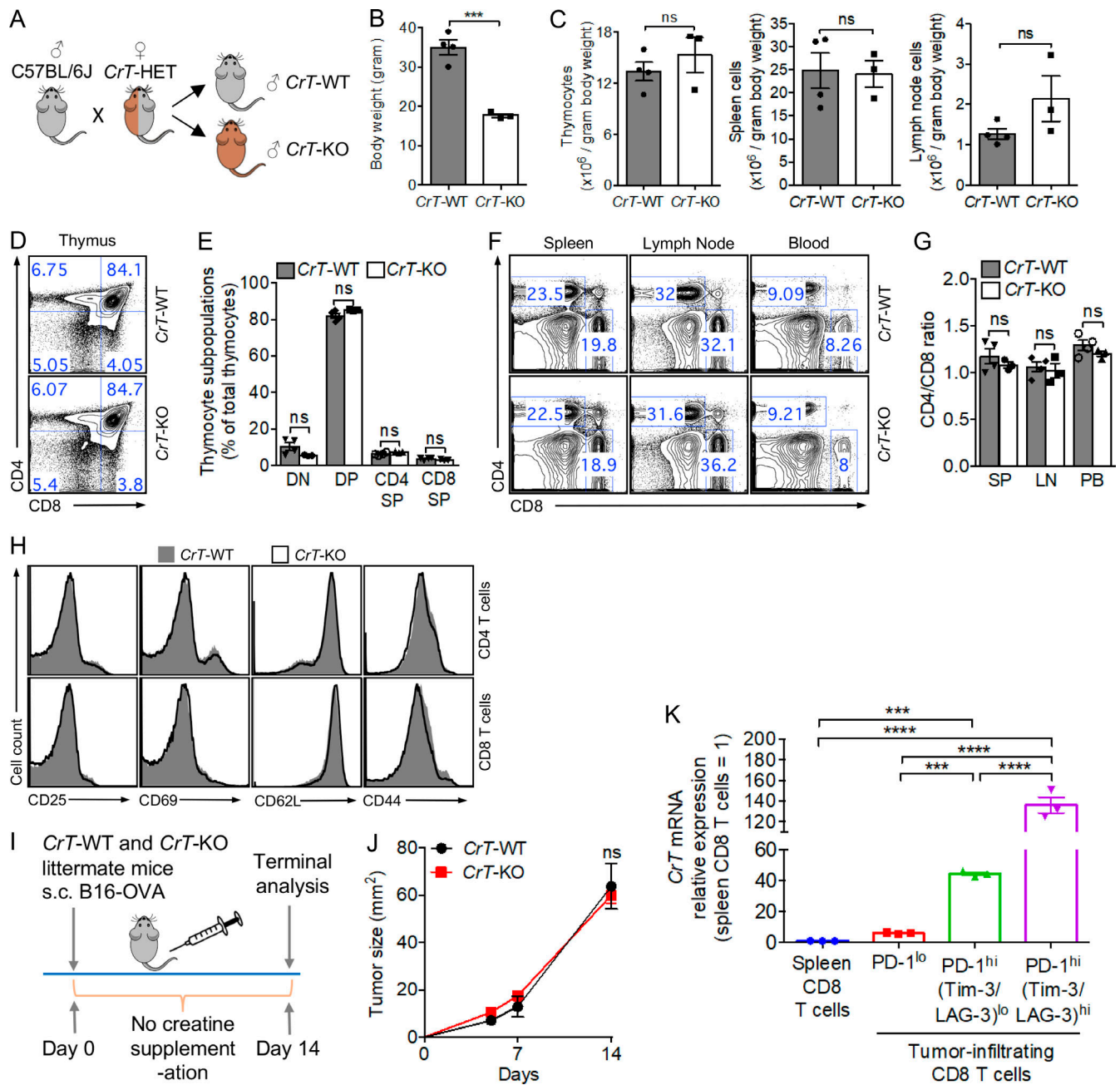
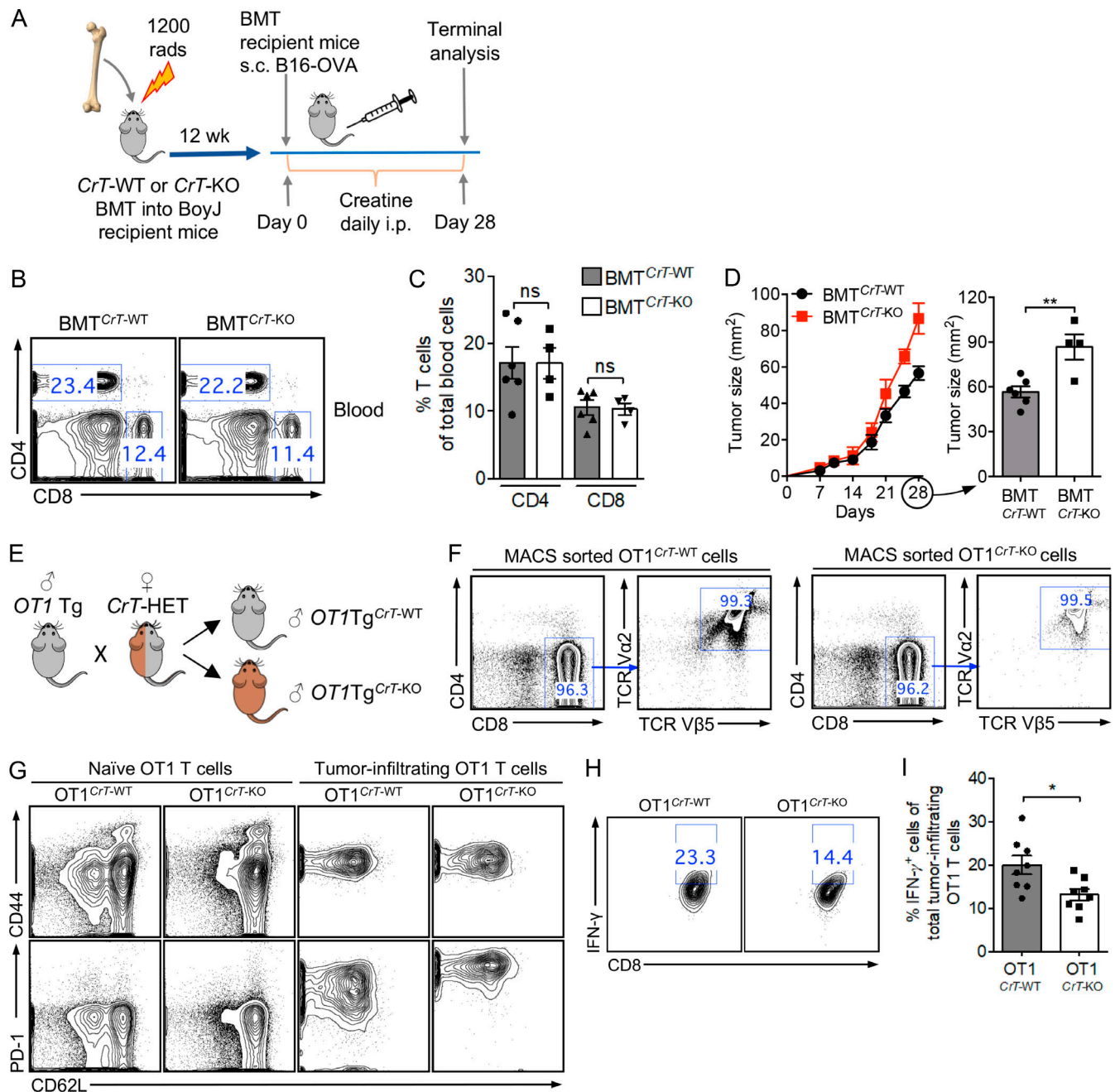


Figure S1. **CrT-KO mice show impeded control of tumor growth.** Related to Fig. 1. **(A–H)** Characterization of CrT-KO mice. **(A)** Breeding strategy for the generation of CrT-KO mice. **(B–H)** Characterization of CrT-KO mice in comparison with their CrT-WT littermate controls ( $n = 3–4$ ). **(B)** CrT-KO mice showed reduced body weight. **(C)** CrT-KO mice contained normal numbers of immune cells proportional to their body weight. **(D and E)** CrT-KO mice showed normal T cell development in thymus. **(D)** FACS plot showing the developmental stages of thymocytes defined by CD4/CD8 coreceptor expression. **(E)** Quantification of D. **(F and G)** CrT-KO mice contained normal levels of CD4 and CD8 T cells in the periphery. **(F)** FACS plots showing the detection of CD4 and CD8 T cells in the periphery. **(G)** Quantification of F. **(H)** Peripheral T cells in the CrT-KO mice displayed a normal naive T cell phenotype (CD25<sup>lo</sup>CD69<sup>lo</sup>CD62L<sup>hi</sup>CD44<sup>lo</sup>). FACS plots of peripheral blood T cells are shown. **(I and J)** Study of B16-OVA tumor growth in CrT-WT and CrT-KO littermate mice without creatine supplementation. **(I)** Experimental design. **(J)** Tumor growth ( $n = 3$ ). **(K)** Study of CrT gene expression in tumor-infiltrating CD8 T cell subsets. B6 mice were inoculated with B16-OVA tumor cells. On day 19, TILs were isolated, and CD8 T cells (pregated as CD45.2<sup>+</sup>TCR $\beta$ <sup>+</sup>CD8<sup>+</sup> cells) were sorted into three subsets: PD-1<sup>lo</sup>, PD-1<sup>hi</sup> (Tim-3/LAG-3)<sup>lo</sup>, and PD-1<sup>hi</sup> (Tim-3/LAG-3)<sup>hi</sup>. CD8 T cells (gated as CD45.2<sup>+</sup>TCR $\beta$ <sup>+</sup>CD8<sup>+</sup> cells) sorted from the spleen of age-matched, tumor-free B6 mice were included as a control. qPCR analysis of CrT mRNA expression in the indicated CD8 T cells is presented ( $n = 3$ ). Representative of two experiments (A–K). Data are presented as the mean  $\pm$  SEM. ns, not significant; \*\*\*,  $P < 0.001$ ; \*\*\*\*,  $P < 0.0001$  by Student's  $t$  test (B, C, E, G, and J), or one-way ANOVA (K).



**Figure S2. Creatine uptake deficiency directly impairs antitumor T cell immunity.** Related to Fig. 2. **(A–D)** Studying B16-OVA tumor growth in BoyJ mice receiving adoptive transfer of BM cells from *CrT*-WT or *CrT*-KO donor mice (BMT<sup>*CrT*-WT</sup> or BMT<sup>*CrT*-KO</sup> mice). **(A)** Experimental design. **(B and C)** Characterization of BMT<sup>*CrT*-WT</sup> and BMT<sup>*CrT*-KO</sup> mice. *CrT* deficiency did not impair the capacity of BM cells to reconstitute the T cell compartment in BoyJ recipient mice. **(B)** FACS plots showing the detection of CD4 and CD8 T cells in blood (gated as CD4<sup>+</sup> and CD8<sup>+</sup> cells, respectively). **(C)** Quantification of B ( $n = 4–6$ ). **(D)** Tumor growth ( $n = 4–6$ ). **(E–I)** Studying the antitumor capacity of *CrT*-WT and *CrT*-KO OT1 Tg T cells (related to Fig. 2, A–H). **(E)** Breeding strategy for the generation of OT1 Tg (*OT1* Tg) mice deficient in *CrT* gene (*OT1*Tg<sup>*CrT*-KO</sup> mice), in contrast to the conventional OT1 Tg mice (*OT1*Tg<sup>*CrT*-WT</sup> mice). **(F)** FACS plots showing the isolation of OT1 Tg T cells (>99% purity, gated as CD4<sup>+</sup>CD8<sup>+</sup>TCR Va2<sup>+</sup>TCR Vb5<sup>+</sup> cells) from *OT1*Tg<sup>*CrT*-WT</sup> mice (*OT1*Tg<sup>*CrT*-WT</sup> cells) and *OT1*Tg<sup>*CrT*-KO</sup> mice (*OT1*Tg<sup>*CrT*-KO</sup> cells) using MACS. **(G–I)** On day 20 after tumor inoculation, B16-OVA tumors were collected from experimental mice, and TILs were isolated for further analysis. OT1 Tg T cells were identified as CD45.2<sup>+</sup>CD8<sup>+</sup> cells. **(G)** Studying the impact of *CrT* deficiency on OT1 T cell infiltration into tumor. Representative FACS plots were presented. Compared with *OT1*Tg<sup>*CrT*-WT</sup> cells, *OT1*Tg<sup>*CrT*-KO</sup> cells displayed a similar antigen-experienced phenotype (CD44<sup>hi</sup>CD62L<sup>lo</sup>) but exhibited a more exhaustion-prone characteristic, as shown by the higher expression of PD-1. **(H and I)** Studying the impact of *CrT* deficiency on functionality of tumor-infiltrating OT1 T cells. **(H)** FACS plots showing the measurements of intracellular IFN- $\gamma$ . Before intracellular cytokine staining, TILs were stimulated with PMA and ionomycin in the presence of GolgiStop for 4 h. **(I)** Quantification of H ( $n = 8$ ). Representative of two experiments (A–I). Data are presented as the mean  $\pm$  SEM. ns, not significant; \*,  $P < 0.05$ ; \*\*,  $P < 0.01$  by Student's *t* test.

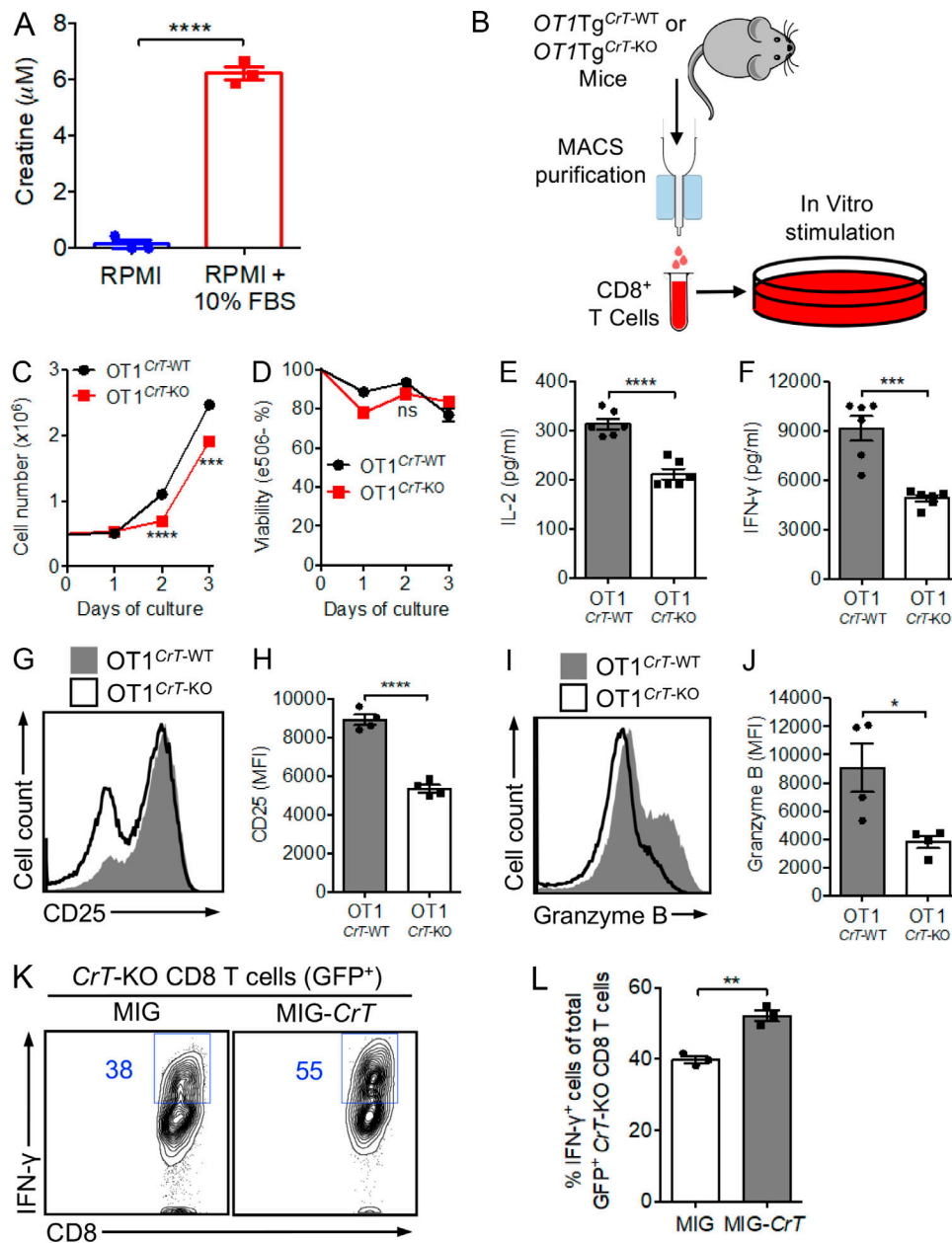


Figure S3. **Creatine uptake regulates CD8 T Cell response to antigen stimulation.** Related to Fig. 3. **(A)** Creatine levels in standard T cell culture medium, measured using a Creatine Assay Kit (Abcam). Note FBS was the source of creatine. **(B–J)** Study of creatine uptake regulation of antigen-specific CD8 T cell response. OVA-specific *OT1* Tg CD8 T cells were isolated from the *OT1Tg<sup>CrT-WT</sup>* or *OT1Tg<sup>CrT-KO</sup>* mice (denoted as *OT1<sup>CrT-WT</sup>* or *OT1<sup>CrT-KO</sup>* cells, respectively) and then stimulated in vitro with anti-CD3. **(B)** Schematic of the experimental design to isolate *OT1<sup>CrT-WT</sup>* and *OT1<sup>CrT-KO</sup>* cells for in vitro stimulation. **(C–J)** The analyses of cell proliferation (C;  $n = 3$ ), cell viability (D;  $n = 4$ ), effector cytokine production (E and F;  $n = 6$ ), surface CD25 activation marker expression (G and H;  $n = 4$ ), and cytotoxic molecule production (I and J;  $n = 4$ ) are shown. Data of E–J were collected at 48 h after stimulation. MFI, mean fluorescence intensity. **(K and L)** Study of *CrT-KO* CD8 T cells transduced with MIG-*CrT* retrovector (related to main Fig. 3, O–S). **(K)** FACS plots showing the intracellular staining of IFN- $\gamma$  effector cytokine in GFP<sup>+</sup> *CrT-KO* CD8 T cells 96 h after anti-CD3 stimulation and MIG-*CrT* transduction. **(L)** Quantification of K ( $n = 3$ ). Representative of two experiments (A–L). Data are presented as the mean  $\pm$  SEM. ns, not significant; \*,  $P < 0.05$ ; \*\*,  $P < 0.01$ ; \*\*\*,  $P < 0.001$ ; \*\*\*\*,  $P < 0.0001$  by Student's  $t$  test.

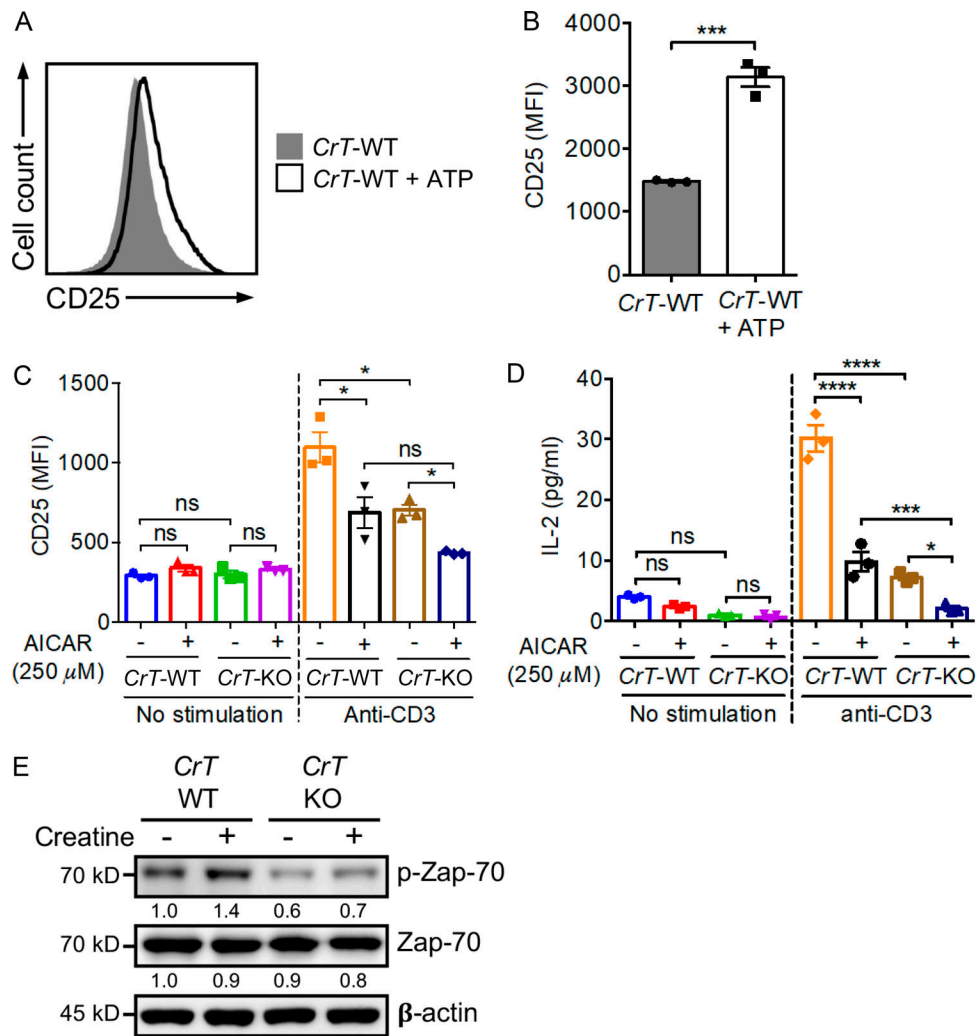


Figure S4. **Creatine uptake regulates CD8 T cell response by regulating T cell ATP/energy buffering.** Related to Fig. 4. **(A and B)** Study of *CrT*-WT CD8 T cell activation with ATP supplementation. *CrT*-WT CD8 T cells were stimulated with anti-CD3, with or without ATP supplementation (100 μM) in the culture medium, and analyzed for surface CD25 activation marker at 48 h. **(A)** FACS plots showing CD25 expression. **(B)** Quantification of A ( $n = 3$ ). Note that ATP supplementation further increased the activation of *CrT*-WT CD8 T cells. MFI, mean fluorescence intensity. **(C and D)** Study of *CrT*-WT and *CrT*-KO CD8 T cell activation with or without AICAR treatment. *CrT*-WT and *CrT*-KO CD8 T cells were pretreated with DMSO or AICAR (250 μM) for 30 min followed by stimulation with anti-CD3 for 16 h. DMSO, solvent used to dissolve AICAR. **(C)** CD25 activation marker expression measured using flow cytometry ( $n = 3$ ). **(D)** IL-2 production measured using ELISA ( $n = 3$ ). **(E)** Study of TCR proximal signaling events in *CrT*-WT and *CrT*-KO CD8 T cells with or without creatine supplementation. Purified *CrT*-WT and *CrT*-KO CD8 T cells were stimulated in vitro with anti-CD3 in the presence or absence of creatine supplementation (0.5 mM) for 48 h, rested at 4°C for 2 h, then restimulated with anti-CD3 in the presence or absence of creatine (0.5 mM) for 10 min. Representative Western blot images showing the analysis of Zap-70 phosphorylation were presented. Representative of two experiments (A–E). Data are presented as the mean ± SEM. ns, not significant; \*,  $P < 0.05$ ; \*\*\*,  $P < 0.001$ ; \*\*\*\*,  $P < 0.0001$  by Student's  $t$  test (B) or one-way ANOVA (C and D).

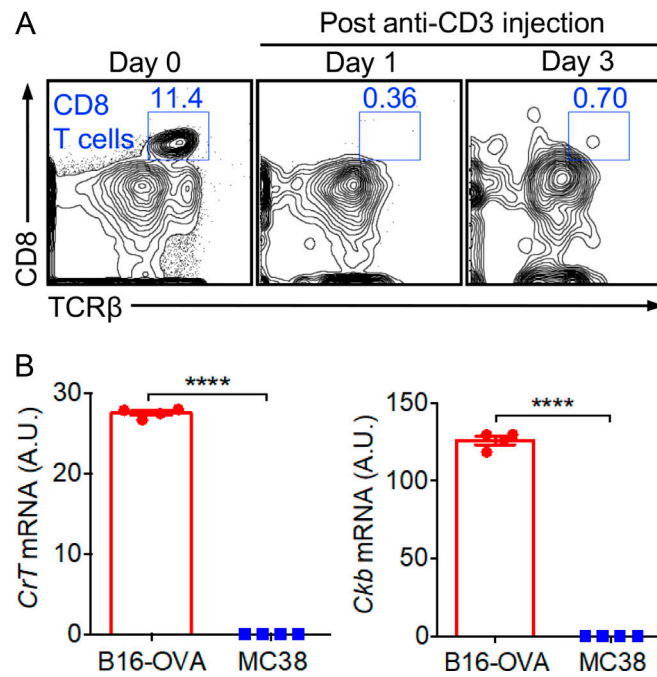


Figure S5. **Creatine supplementation for cancer immunotherapy.** Related to Figs. 5 and 6. **(A)** Studying the requirement of T cells for cancer therapy effects (related to Fig. 5, J and K). Anti-CD3 monoclonal antibody ( $\alpha$ CD3, clone 17A2) was used for in vivo depletion of T cells. FACS plots are presented showing the depletion of T cells, in particular CD8 T cells (gated as  $\text{TCR}\beta^+\text{CD8}^+$ ), in peripheral blood of experimental mice after receiving i.p. injection of anti-CD3. **(B)** Studying *CrT* and *Ckb* mRNA expression in B16-OVA and MC38 tumor cells using qPCR.  $n = 4$ . A.U., artificial unit relative to *Actb*. Representative of two experiments (A and B). Data are presented as the mean  $\pm$  SEM. \*\*\*\*,  $P < 0.0001$  by Student's *t* test.